SIMULATIONS AND DETECTOR TECHNOLOGIES FOR THE BEAM LOSS MONITORING SYSTEM AT THE ESS LINAC

I. Dolenc Kittelmann*, T. Shea, ESS, Lund, Sweden

Abstract

The European Spallation Source (ESS), which is currently under construction, will be a neutron source based on 5 MW, 2 GeV superconducting proton linac. Among other beam instrumentation systems, this high intensity linac requires a Beam Loss Monitoring (BLM) system. An important function of the BLM system is to protect the linac from beam−induced damage by detecting unacceptably high beam loss and promptly inhibiting beam production. In addition to protection functionality, the system is expected to provide the means to monitor the beam losses during all modes of operation with the aim to avoid excessive machine activation. This paper focuses on the plans and recent results of the beam loss studies based on Monte Carlo (MC) simulations in order to refine the ESS BLM detector requirements by providing the estimations on expected particle fluxes and their spectra at detector locations. Furthermore, the planned detector technologies for the ESS BLM system will be presented.

INTRODUCTION

The ESS is a material science facility, which is currently being built in Lund, Sweden and will provide neutron beams for neutron−based research [1]. The neutron production will be based on bombardment of a tungsten target with a proton beam of 5 MW average power. A linear accelerator (linac) [2] will be used to accelerate protons up to 2 GeV and transport them towards the target through a sequence of a normal conducting (NC) and superconducting (SC) accelerating structures (Fig. 1).

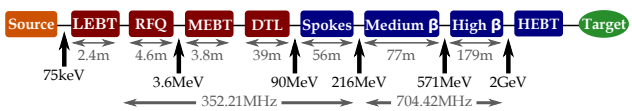

Figure 1: The ESS linac layout. Red color represents the NC and blue the SC parts of the linac.

Rapid startup and reliable operation of the linac requires a certain suite of beam instrumentation. As part of this suite, the BLM system will detect high beam losses potentially harmful to the linac components and inhibit beam production before damage occurs. Additionally, the system provides information about the particle rates during all linac modes of operation in order to enable tuning and keep the machine activation low enough for hands−on maintenance.

ESS BLM DETECTOR TECHNOLOGIES

The ESS BLM system will employ 3 types of detectors. In the SC parts of the ESS linac, parallel plate gas ionization chambers (ICs) developed for the LHC BLM system [3] will be used (Ionization Chamber based BLM − ICBLM). These were chosen due to their availability as part of a joint procurement with CERN and other facilities. Background due the RF cavities must be taken into account when using ICs in a linac. This background is mainly due to the electron field emission from cavity walls resulting in bremsstrahlung photons created on the cavity or beam pipe materials [4]. The background levels are difficult to predict numerically as they depend on the quality of the cavities, beam loading, operation conditions and time. It is planned to asses this experimentally at the ESS RF test stand in Uppsala with the spoke cavities and at the CEA Saclay with the elliptical cavities. Nevertheless, simplified energy spectra estimations show that photons with energies up to tens of MeV can be expected [5]. With a characteristic cut−off value for the photons of ∼2 MeV for the LHC ICs [3], background sampling and subtraction is needed for the ICBLM system. In addition to the primary IC-based system, some Cherenkov radiation detectors may also be deployed. These offer inherent rejection of the RF cavity background.

BLM detectors are planned also in the MEBT and DTL sections of the NC ESS linac. Here the particle fields outside the tanks and beam pipe are expected to be dominated by the neutrons and photons. With RF cavity background still a possible source of photons in these sections, a neutron sensitive detector should be considered. Special micromegas detectors are in development [6] by the micromegas team from the CEA Saclay, designed to be sensitive to fast neutrons, but not to thermal neutrons, X−rays or γ−rays.

ESS BLM SIMULATIONS

MC simulations for tracking of the lost protons are needed in order to address several points crucial for the design of a BLM system, namely: system response time limit, detector locations and dynamic range of the system. In addition to this, they provide a tool for determination of the initial machine protection threshold settings used during the startup period. Furthermore, the MC simulations serve to estimate the anticipated response of the system during the fault studies that will verify the BLM system response. The focus of this chapter are the aforementioned first three simulation tasks, while the last two are not discussed here.

Most of the results presented here are focused on the NC linac, and will provide a basis for the nBLM specifications. The anticipated neutron and photons spectra at the detector locations are required to finalize the micromegas detector design. Previous efforts focused primarily on the SC linac; thus some preliminary results valid for the ICBLM already exist.

* irena.dolenckittelmann@esss.se

ISBN 978-3-95450-178-6

The Geant4 (version 10.00.03, QGSP_BIC_HP physics list) simulation framework [7] developed by the ESS neutron detector group has been used to perform the ESS BLM simulations. No tracking cuts have been employed, while production cuts were set to 10 µm for e^+, e^- and photons.

A Geant4 based ESS linac geometry (Fig. 2) has been created with certain element models (quadrupole magnets, spoke and elliptical cavities and mid parts of the elliptical cryomodules) adapted and changed where needed from the existing ROOT [9] based ESS linac model used for shielding calculations [10]. Magnetic field maps [11] outside the beam pipe for the quadrupole magnets in the SC linac are included in the simulation due to their important impact on the simulation results for the detectors placed close to the these magnets. The linac elements' apertures, lengths and positions follow the values in the 2015 baseline beam physics lattice of the ESS linac. Due to their importance for the low energy parts of the neutron spectra, tunnel walls are included in the simulations. Current simplifications to the geometry include:

- Simplified quadrupole magnet geometry in the yoke and coil length.
- Simplified model of the DTL gaps, where 1−2 cylindrical shapes on each side of the gap are used. The value of (gap length)/(cell length) is the same for all cells in one tank and taken as the average value in the tank.
- Model for cavities in HB sections is calculated by scaling part of the MB cavity profile.
- The following elements are currently not included: post−couplers in the DTL, beam instrumentation devices, correctors, supports, MEBT chopper and chopper dump, spoke cavity insertions.

Certain set of inputs are needed in order to perform the BLM simulations. Ideally one would have a list of accidental beam loss scenarios with corresponding loss maps together with a list of the elements that must be protected along with their damage thresholds. In addition to this, the anticipated loss maps during the normal operation are needed as the lowest detectable BLM signal levels are expected during these periods. However, due to the large number of possible accidental scenarios and operating conditions, some simplifications and assumptions are needed. These are considered in the following subsections in connection to the discussions of the worst case accidental beam loss scenario and detector locations.

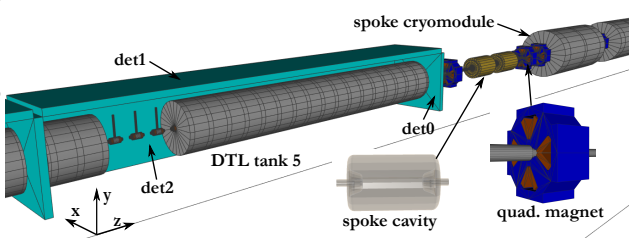

Figure 2: Geant4 based geometry of the ESS linac used in the BLM simulations, focused on the last tank of the DTL section. Phantom detector modules surrounding the tank are marked as det0, det1 and det2. Parts of the volumes are opened for a better view.

Response Time

The required response time of the BLM system was set in the past to ∼5 µs in the NC (MEBT and DTL) and ∼10 µs in the SC parts of the linac [12]. The numbers are based on simplified melting time calculations, where a beam of protons with a uniform profile hits a block of material under perpendicular incidence angle. No cooling is considered in these calculations. The numbers have recently been checked with the updated beam parameters and a Gaussian beam profile. These results support the 10 µs requirement in the SC parts of the linac, and as mentioned below, other damage mechanisms to the SC cavities may mandate an even lower latency. In the NC section, the calculated melting time values of 3−4 µs imply even stronger demands on the response time (Fig. 3). The latter has additionally been confirmed with a MC simulation.

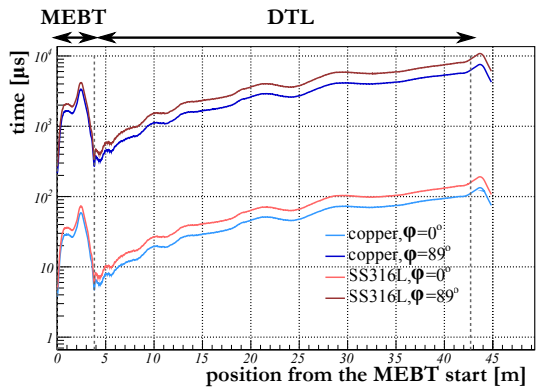

Figure 3: Time to melt a block of copper (blue) or stainless steel (red) under constant irradiation with a proton beam under perpendicular incidence (φ=0°) or a very shallow angle.

Worst case accidental beam loss scenario Melting time depends on the beam incidence angle; thus, the validity of the assumption of the perpendicular incidence as the worst case scenario can be argued. This poses a question on what the worst case accidental loss is, which translates to the need to understand what is the least shallow incidence angle of the most focused beam that can be expected to hit the aperture. This is expected to occur for a particular case of incorrect settings for a set of corrector magnets. Time consuming beam dynamics simulations are required in order to asses this. Therefore the following strategy to find the worst case angle has been suggested [13] and adopted here:

- Increase one of the initial coordinates x, x', y or y' at the beginning of a linac section until the beam centroid starts touching the aperture.

ISBN 978-3-95450-178-6

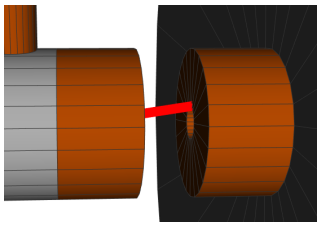

Figure 4: Example of beam hitting a tube in the DTL tank 1 (incidence angle set to 150 mrad).

- The highest deflection found along the section is taken as the worst case angle.

An assessment of this type has been performed [13] for the DTL and HEBT sections (Table 1).

Table 1: Worst Case Beam Incidence Angle (Courtesy of R. Miyamoto)

ESS Linac section	Peak x' or y' [mrad]
DTL tank 1	50
DTL tank 2–3	15
DTL tank 4–5	10
HEBT	20

Implications on the response time Depending on the gap distance, an incidence close to perpendicular is potentially possible in the first DTL tank due to the almost flat surfaces between the gaps (Fig. 4). Given the worst case angle as currently understood, this is geometrically possible though highly improbable as it requires the incidence angle larger than about 3 times the worst case one in the simplified DTL geometry used in the BLM simulations. This deserves further studies with a more accurate mechanical model of the DTL.

In order to determined the time response limit in the SC sections, it is foreseen to check the beam pipe melting time with a focused beam under worst case angle discussed above. However a degradation of the cavities is observed at the SNS after losing a <15 µs pulse of 26 mA beam about 10 times per day [14]. This motivates setting the response time limit for the ESS SC linac significantly lower than 15 µs.

Detector Locations

The most suitable set of detector locations and their count ensures that the system is not blind to any of the accidental losses. In the absence of a complete list of accidental losses, the following strategy is assumed in order to select detector locations:

- A set of localized loss scenarios is considered, each with a selected beam energy, incidence angle and loss location along the linac section under investigation.
- The incidence angle is varied from ∼1 mrad up to the worst case angle as discussed in the previous subsection, while the lost proton energy is varied from the lowest anticipated to the nominal value. The lowest anticipated energy depends on the section in question and is planned to be assessed in the near future.
- By using phantom detectors (with vacuum as the volume material) surrounding the section, a simulation for each of the loss scenarios is run to produce hit maps of incoming neutrons (in case of nBLM) or all particles (in case of ICBLM).
- Hit map mean and RMS values along the section length are extracted for each of the loss scenarios and compared with the origin of the loss. The best detector locations can be extracted by comparing the results from all simulation runs.

A strategy for selecting the detector locations based on optimization methods combined with genetic algorithms has been tried in the past, though only for the case of the ICBLMs. It is planned to augment this work in the near future with the above mentioned strategy, however as previously mentioned, the current efforts are focused on the nBLMs due to the need to develop specifications for this detector design.

As an example, some preliminary hit maps are presented in Fig. 5 for two detector volumes placed around the DTL tank 1. Here, a focused beam was generated at 3 different locations along the tank. A beam angle of 50 mrad with respect to the z−axis was selected while the nominal energy at the loss location was taken as the proton energy. The mean values along the z−axis agree to ∼0.02−0.8 m with the loss location for both of the detectors, while RMS values of ∼1.4.−1.5 m are observed. The same observations holds if a detector volume is placed below the tank, though as expected, this detector yields the lowest hit rate. These results look promising in the view of the BLM system's capability to localize the loss locations, and they justify the need for further simulation.

Dynamic Range

Once the detector locations are known, the dynamic range of the BLM system can be determined by studying two extreme cases:

- **Highest expected hit rate.** This case marks the worst case accidental loss. By assuming the worst case angles discussed in subsection focused on the response time, the simulated particle hit rate can be used to estimate the upper limit of the system's dynamic range.
- **Lowest expected hit rate.** Typically the lower limit of a BLM system dynamic range is set to a fraction of a 1 W/m, which is arguably coming from the activation limit for the hands−on maintenance. To support tuning and optimization, it is also useful to asses the expected signals for example operating scenarios, when certain areas may have loss levels well below the activation

ISBN 978-3-95450-178-6

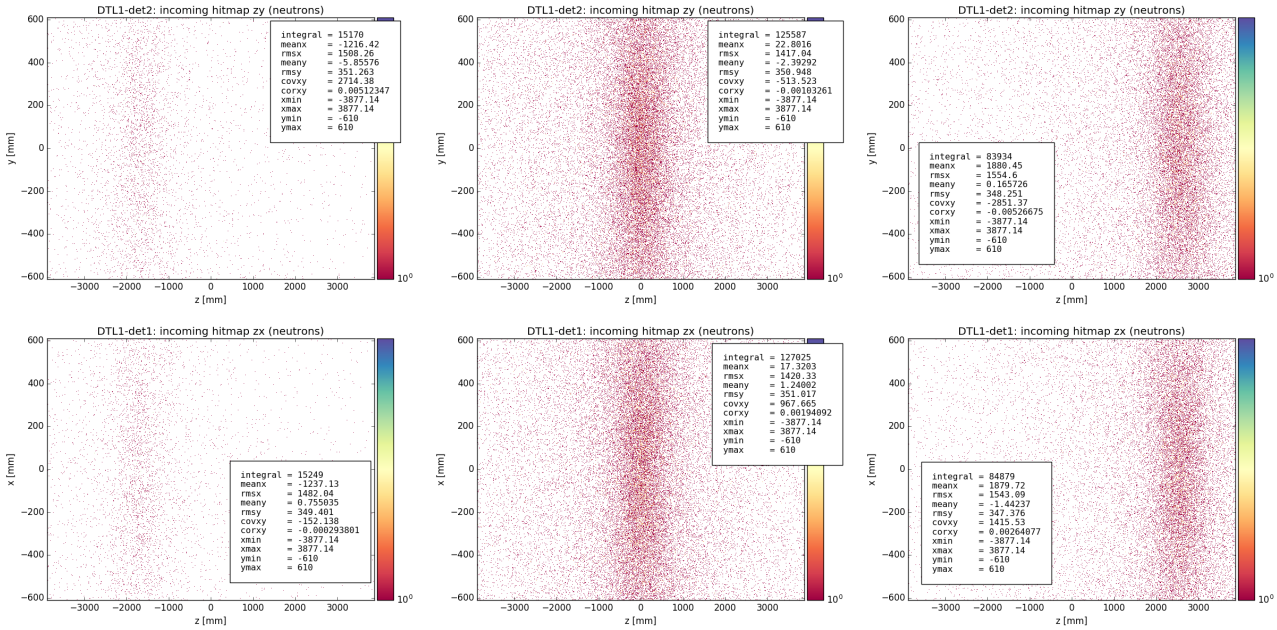

Figure 5: Simulated neutron hit maps for 3 different loss locations along the DTL tank 1 scored in detector volumes det2 (top) and det1 (bottom). See Fig. 2 for the detector locations.

limit. The lower end of the dynamic range can than be set to a fraction of this signal.

Expected loss map during normal operation Beam dynamics error studies have been performed on the 2015 baseline beam physics lattice of the ESS linac [15, 16]. Here the errors were applied to 10000 machines, each with 600000 macro−particles. The error tolerances were set to 100 % of the nominal values, except for the dynamic error (RF jitter), where it was increased to 200 %. The results of this study (Fig. 6) are used as the input to the BLM MC simulation of lost protons and are assumed to represent a realistic scenario of ESS linac beam loss during normal operation.

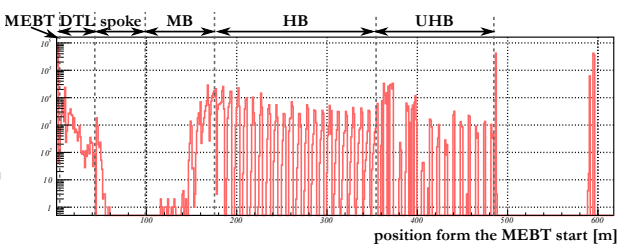

Figure 6: Distribution of the lost protons along the ESS linac resulting from the ESS linac error study [15, 16], which served as an input loss map for the BLM simulation of the linac normal operation.

Normal operation versus 1W/m loss In order to assess the difference between the normal operation and 1 W/m loss, BLM MC simulations of lost protons have been performed for both cases with the following settings:

- **Normal operation loss.** Lost protons were sampled from the lost particle distributions (azimuth and polar angle of the particle momentum, azimuth angle of the particle position and particle energy) obtained from the aforementioned mentioned error study. This approach offers no limitation on the statistics of the BLM simulation and no need for assumptions on the lost particle distributions. Correlation was observed between the azimuth angles for the lost proton position and momentum direction, which was taken into account in the simulation as well.

- **1 W/m loss.** A uniform distribution of lost protons was assumed along the linac. Particle momentum polar angle from the beam axis was fixed to 1 mrad while the particle position azimuth angle was sampled uniformly around the aperture. Particle energy was set to the nominal value at the lost proton location.

The linac geometry used included MEBT and DTL sections together with the first 4 cryomodules of the Spoke section.

The simulated neutron spectra in units of neutrons/s hitting a detector volume for the case of the normal operation and 1W/m loss in the DTL tanks are shown on Fig. 7. For the case of the uniform loss, an increase in incoming neutrons with the tank number is observed which can be attributed to the increase of the neutron production cross−section with increasing proton energy. On the other hand, the normal operation results exhibit the lowest neutron fluxes in the last two tanks. The latter can be explained by emittance decrease with increasing beam energy. By comparing the results for the two loss scenarios, it can be seen that all 1 W/m spectra

ISBN 978-3-95450-178-6

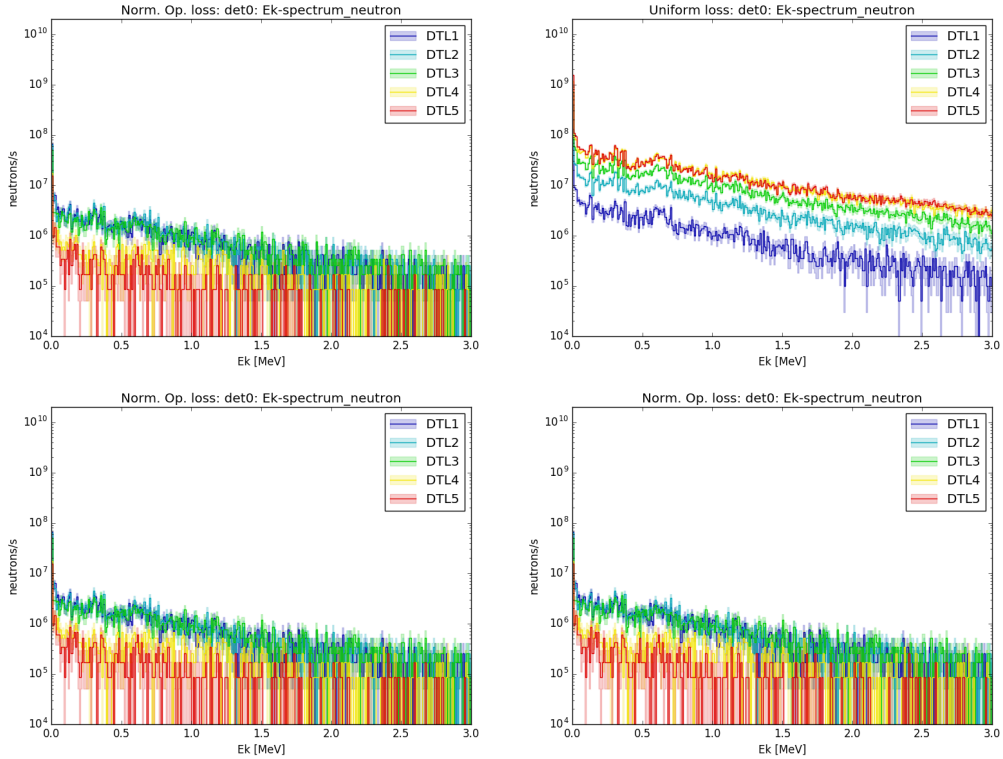

Figure 7: Simulated neutron energy spectra hitting the detector volume det0 (top) and det1 (bottom) for the case of normal operation (left) and 1W/m (right) loss. Different color marks the different DTL tank. See Fig. 2 for the detector locations.

lie above the corresponding ones for the case of normal operation. The difference increases with the tank number from 0 to ~1.5 order of magnitude. The exception is the det0 in the DTL tank1, where the 1 W/m curve is approximately similar to or lies slightly below the corresponding normal operation results.

Dynamic range specification Following the discussion above, once the nBLM detector locations are fixed, the lower limit of the dynamic range for the case of the nBLMs can be set to a fraction of the neutron flux expected during the normal operation. The upper limit on the other hand can be estimated by assuming total beam loss. Since protection should be provided under conditions with maximum damage potential, a focused beam under worst case incidence angle is assumed.

For the case of the ICBLMs, preliminary values have been set in the past [17] by requiring the BLM to able to measure 1 % of the 1 W/m loss during normal operation and up to 1 % of the total beam loss. This gave an estimation for the IC output current range, which was found to be from ~800 mA to few mA. It is planned to re−asses these values in the near future once the ICBLM detector locations are set as well.

SUMMARY

The 3 types of detector technologies planned for the ESS BLM system were presented. In SC parts of the linac ICs will be used as the primary BLM detectors (ICBLMs). It is foreseen to explore an option to use a Cherenkov radiation sensitive detectors as complementary BLMs to the ICBLMs in the SC parts. The advantage of these detectors lies in their low sensitivity to the RF cavity background. On the other hand, novel neutron sensitive micromegas detectors will be used as the BLMs in the NC parts of the linac.

The second part of the paper was focused on the MC simulations of lost protons, which are a necessary tool when building a BLM system. In the past all simulation efforts were focused on the SC linac. Currently the focus has turned to the NC parts due to the need for the inputs in order to design the nBLM detectors.

Strategies to determine the specifications (response time, dynamic range and detector location) of the ESS BLM system were discussed. Selected preliminary results for the NC linac parts were presented together with the past results which were exclusively focused on the SC linac.

ACKNOWLEDGEMENT

The authors would like to thank M. Eshraqui, Y.I. Levinsen and R. Miyamoto (ESS) for their help in the form of beam physics discussions and studies needed to perform the BLM MC simulations. Additionally the authors wish to thank R. de Prisco (ESS) and I. Tropin (FNAL) for the help with the ESS linac geometry. Authors are also thankful to T. Kittelmann (ESS) for providing the support with the Geant4 computing framework.

ISBN 978-3-95450-178-6

REFERENCES

[1] "ESS: Technical Design Report", ESS report ESS-0016915 (2013).

[2] M. Eshraqi *et al.*, "The ESS Linac", in *in Proc. IPAC'14*, Dresden, Germany, paper MOXAP07.

[3] M. Stockner *et al.*, "Classification of the LHC BLM Ionization Chamber", in *Proc. DIPAC'07*, Venice, Italy, paper WEPC09.

[4] E. Donoghue *et al.*, "Studies of Electron Activities in SNS-Type Superconducting RF Cavities", in *Proc. SRF'05*, Ithaca, NY, USA, paper TUP67.

[5] B. Cheymol, "ESS wire scanner conceptual design", ESS report ESS-0020237 (2016).

[6] T. Papaevangelou, "Micromegas detector applications for beam diagnostics", CERN BI seminar, CERN, Geneva, Switzerland (2016), http://indico.cern.ch/event/540799/

[7] T. Kittelmann *et al.*, "Geant4 Based Simulations for Novel Neutron Detector Development" CHEP 2013, Amsterdam, Netherlands (2013), doi:10.1088/1742-6596/513/2/022017, http://iopscience.iop.org/article/10.1088/1742-6596/513/2/022017/meta

[8] GEANT4 collaboration, http://geant4.web.cern.ch/geant4

[9] https://root.cern.ch/

[10] N. Mokhov *et al.*, "ESS accelerator prompt radiation shielding design assessment", ESS report ESS-0052477 (2016).

[11] ESS reports ESS-0040133, ESS-0040134

[12] L. Tchelidze, "How Long the ESS Beam Pulse Would Start Melting Steel/Copper Accelerating Components?", ESS report ESS/AD/0031 (2012) http://docdb01.esss.lu.se/DocDB/0001/000168/001/Time_Response_Requirements_BLM.pdf

[13] R. Miyamoto, private communication.

[14] W. Blokland *et al.*, "A new differential and errant beam current monitor for the SNS accelerator", in *Proc. IBIC'13*, Oxford, UK, paper THAL2.

[15] Y.I. Levinsen, "ESS 2015 Baseline Lattice Error Study", ESS report ESS-0049433 (2016).

[16] Y.I. Levinsen *et al.*, "Beam Dynamics Challenges in the ESS linac", presented at HB'16, Malmö, Sweden, paper TUAM3Y01.

[17] L. Tchelidze *et al.*, "Beam Loss Monitoring at the European Spallation Source", in *Proc. IBIC'13*, Oxford, UK, paper WEPC45.

ISBN 978-3-95450-178-6